Available online at www.sciencedirect.com
ScienceDirect
Digital Signal Processing 17 (2007) 965–978
Digital Signal Processing
www.elsevier.com/locate/dsp

Processing the acute cocaine FMRI response in human brain with Bayesian source separation

Peter R. Kufahl [a], Daniel B. Rowe [b,c,*], Shi-Jiang Li [c]

[a] *Department of Psychology, Arizona State University, Tempe, AZ, USA*
[b] *Division of Biostatistics, Medical College of Wisconsin, Milwaukee, WI, USA*
[c] *Department of Biophysics, Medical College of Wisconsin, Milwaukee, WI, USA*

Available online 23 March 2007

Abstract

Pharmacological FMRI in humans involves BOLD signal acquisition before, during and after the administration of a drug, and often results in a heterogeneous pattern of drug-induced hemodynamic responses in the brain. Exploratory techniques, including blind source separation, can be useful for BOLD data that contains patterns of cross-dependencies. Bayesian source separation (BSS) is a multivariate technique used to calculate the presence of unobserved signal sources in measured FMRI data, as well as the covariance between data voxels and between reference waveforms. Unlike conventional univariate regression analysis, BSS does not assume independence between voxel time series or source components. In this study, BOLD measurement of the acute effect of an intravenous dose of cocaine, a substance shown previously to engage multiple sites within the orbitofrontal cortex, was processed with BSS. The utility of BSS in pharmacological FMRI applications was demonstrated in multiple examples featuring single-ROI, multiple-ROI and whole-slice data. The flexibility of the BSS technique was shown by choosing different modeling strategies to form the prior reference functions, including approximating the pharmacokinetics of cocaine, interpolating simultaneously measured behavioral data and using observed BOLD responses from known subcortical afferents to the cortex of interest.

Keywords: Bayesian source separation; Brain; FMRI; Imaging; Cocaine; Multivariate

1. Introduction

Reward processing in humans has been a subject of intense functional magnetic resonance imaging (FMRI) investigation since the primary experiments of direct activation of proposed reward-processing brain circuits by cocaine [1] and nicotine [2]. The data collected in these experiments comprised of thousands of blood-oxygenation level-dependent (BOLD) time series simultaneously acquired from the conscious human brain. Significant changes in BOLD signal magnitude following infusion of a psychoactive drug were judged to be directly related to drug-induced neural responses. The loci of cocaine- or nicotine-induced neural activity were characterized by simultaneous testing of the signal time series, each belonging to a oblong "voxel" within the brain tissue [1–3]. BOLD data has been typically analyzed by comparing individual voxel time series acquired from test and control states with paired t-tests, or

* Corresponding author. Fax: +414 456 6512.
E-mail address: dbrowe@mcw.edu (D.B. Rowe).

1051-2004/$ – see front matter
doi:10.1016/j.dsp.2007.03.001

by correlating the voxel time series with reference waveforms, and generalizing the results by transforming them into z-scores (for example, see [4,5]).

The processing strategies of BOLD data in the studies described above established the feasibility of FMRI measurement of acute psychoactive drug responses in dependent subjects [6], but assumed independence among the BOLD time series of voxels and therefore could not statistically categorize the data into component networks. We used a Bayesian multivariate technique [7] to process the acute BOLD response to an intravenous dose of cocaine measured in a cocaine-addicted human subject, estimating dependencies between voxels residing within cocaine-sensitive regions.

Most FMRI data is currently processed as a set of independent voxelwise tests, resulting in the multiple comparisons problem. Statistical thresholds are often chosen to control the familywise error rate (FWE) or false discovery rate (FDR) in FMRI [8]. The most common and easiest way to control the FWE is with the application of the Bonferroni threshold. However, the Bonferroni technique is very conservative and other methods can be applied to sharpen the FWE threshold. A popular strategy for choosing a workable FWE threshold of voxelwise tests, made popular in low-resolution PET experiments, is to preprocess FMRI data using the concepts of Gaussian random field theory [9]. FMRI data is assumed to have an intrinsic smoothness approximating that of a continuous random field. This assumption is ensured by spatially blurring the data to at least twice the acquired voxel size, somewhat compromising the spatial resolution advantage of FMRI. Another strategy is to utilize permutation resampling to determine a FWE threshold. One can also assess the statistical map in terms of clusters, where adjacent voxels that pass the voxelwise threshold belong to the same cluster. Clusters of a given size are then required to pass the overall threshold of significance, determined by simulation and dependent on spatial blurring and total number of voxels being tested [10]. Since cocaine has been shown to activate voxels in both cortical areas and subcortical areas of the human brain in FMRI studies [1,3], the sizes of statistical clusters are thought to be highly variable. Therefore, the visibility of significant BOLD changes is a function of location within the brain, as well as the voxel-wise and corrected thresholds. For this reason, we elected to minimize the spatial blurring in the preprocessing stages of analysis, and not use the concepts of Gaussian random field theory.

The observation that cocaine induces multiple well-recognized processes in addicts, described as "liking" and "wanting" in the literature, and the notion that different networks of brain regions may be responsible for the drug-induced relapse [11], inspires a view of FMRI data as a mixture of a limited number of unobserved sources, rather than a set of thousands of independent BOLD measurements. If the p-dimensional set of voxel time courses were to be reduced to a much smaller number of underlying signal sources, $q \ll p$, then the sources could be inferred to correspond to discrete mental processes of the subject. Kufahl and colleagues [3] demonstrated the limited separability of *high*- and *craving*-related BOLD data by univariate processing (for two loci in the OFC, at least 6 out of 9 subjects exhibited BOLD responses significantly correlated to both *high* and *craving* VAS ratings), and the consequently incomplete localization of cocaine "wanting" and "liking."

Multivariate analysis methods have been developed to analyze FMRI data, essentially decomposing p BOLD time series into $q < p$ underlying "components" of interest, without assuming mutual independence between voxel time courses [12]. The principal task of these methods is to reduce the dimensionality of the analysis from p to q by imposing constraints on the components for indentifiability [13]. Principal component analysis assumes that components are mutually orthogonal [14], factor analysis assumes uncorrelated components [13], and temporal independent component analysis (ICA) assumes that the components are mutually independent [15]. Since the measured *high* and *craving* ratings only significantly change following cocaine infusion and not saline infusion for the same subjects [3], it is difficult to justify treating cocaine-induced euphoria and craving as orthogonal or independent processes. Although these processes have been shown to correlate with different brain regions in varying levels [1,3], cocaine-induced euphoria and craving are thought to be codependent to some degree [16].

There has been much interest in utilizing Bayesian methodology for informed separation of components [17]. Multivariate analysis that does not impose restrictions of independence on the p observed BOLD time series or the q underlying unmixed BOLD signal sources can be made tractable by formally incorporating prior knowledge about the FMRI experiment, as in a Bayesian framework [18,19].

Bayesian statistics is centered around the use of Bayes' rule, where the posterior probability distribution of a parameter (for a FMRI voxel time series, this might be the regression coefficient to the stimulus) is derived from the prior distribution of that parameter (assessed empirically or otherwise) and the likelihood distribution of the data, given the value of that parameter [20,21]:

$$\text{posterior} \propto \text{likelihood} \times \text{prior}.$$

In the case of analyzing the acute cocaine effect with FMRI, the prior distribution contains information about the absorption and clearance of cocaine in the bloodstream, in the form of a pharmacokinetic model. Prior distributions are also formed for the regression coefficients (in the case of low or nonspecific expectations, large variance terms are used). The likelihood is the distribution of the data, in terms of the parameters that describe the pharmacokinetic model, as well as other possible contributions (linear trend and constant offset). After combining the joint prior and the likelihood with Bayes' rule, a joint posterior distribution for the regression coefficients and the parameters of the pharmacokinetic reference function is found.

The acute effects of cocaine on the human brain have been studied with FMRI, though with either no reference function [1] or an *a priori* fixed reference function [3]. The single-dose pharmacokinetics of a psychoactive drug has been used to produce a differential exponential model for the expected BOLD response, but without region-specific characterization [22].

In this study, BOLD measurement of the acute effect of a dose of cocaine was processed with Bayesian source separation to find activation maps and intervoxel correlation statistics. The generation of t-scores and z-scores, which are often utilized in neuroscience to compare the results of FMRI and other procedures, was also demonstrated. Analysis was restricted to the orbitofrontal cortex (OFC), a relatively heterogeneous paralimbic region of the brain activated by cocaine [3]. The OFC, the ventral surface of the human forebrain, is the subject of intense investigation in multiple neuroscience disciplines [16]. Since the noise characteristics of OFC BOLD data area are heavily influenced by static magnetic field gradients present in the lower brain, specialized MRI acquisition strategies have been developed to compensate for them [23]. Data from an actual FMRI experiment is used to demonstrate Bayesian source separation, instead of a simulation that attempts to replicate these circumstances.

2. Theory

Bayesian source separation (BSS) is a multivariate technique used to statistically determine an unobserved reference function in measured FMRI data, using both the data and a stochastic model of the reference function [18]. BSS was preceded by published applications of Bayesian methodology into ICA signal unmixing, incorporating prior information toward the estimation of the number of sources and error evaluation [24–26]. The mechanics of BSS have been recently developed in implementable detail [7,27].

The Bayesian hemodynamic drug response model (Eq. (1)) describes the FMRI signal of a given region of interest (ROI) with p voxels over n time measurements.

$$Y = XB' + E. \tag{1}$$

The $n \times p$ matrix Y represents the measured FMRI data. The columns of Y are voxel time series made up of sequential BOLD observations. The $n \times (q+2)$ design matrix $X = (X_1, r)$ is composed of observed sources X_1, a constant offset term (first column) and a linear trend (second column), and the pharmacokinetic reference function r (last column). The values of r are considered estimated BOLD amplitudes over time. The columns of X_1 account for the baseline and long-term drifts in the BOLD signal, which are well-known nuisance terms in FMRI [28]. B' is the mixing matrix for the observed sources (the nuisance terms in X) and the unobserved source (r). The sum $q+2$ is the number of regressors in the analysis (there is one regressor for each source), where q is the number of reference functions (in this case, one). The regression coefficients are represented by the $(q+2) \times p$ matrix $B' = (B'_1, B'_2)$, where B_1 corresponds to X_1 and B_2 corresponds to r. The $n \times p$ error matrix E allows dependencies between voxels of the ROI. The $p \times 1$ error vector for each time point ε_t (being the ith row of E) is considered to have the multivariate normal distribution, with zero mean and $p \times p$ variance-covariance matrix Σ.

The hemodynamic reference function r is not exactly known,[1] and is considered the unobserved source. The available information about r is quantified with a prior multivariate normal distribution (Eq. (2A)) whose mean $r_0(t)$ is given by a model of the neural source of the hemodynamic response (e.g., the single-dose pharmacokinetic model of intravenous cocaine [22]). The *a priori* variance of r, δ, is quantified with an inverted Gamma distribution (Eq. (2B)) whose parametric values (mean and variance) are both determined as the maximum difference between the signal peak and the baseline from the ROI timecourses Δ. Examples described later utilize different strategies for determining r,

[1] The reference function r would be assumed to be fixed and exactly known (no variance) in non-Bayesian analysis, such as general linear modeling by SPM.

including simultaneously measured FMRI or behavioral data. The prior distributions for r (Eq. (2A)) and δ (Eq. (2B)) are conjugate priors [7].

$$p(r|\delta) = (2\pi)^{-n/2}(\delta)^{-n/2}e^{-(r-r_0)'(\delta I_n)^{-1}(r-r_0)/2}, \tag{2a}$$

$$p(\delta) = k_\delta(\delta)^{-\eta/2}e^{-\mathrm{tr}(\delta)^{-1}\Delta/2}. \tag{2b}$$

In Eq. (2A), I_n is an n-dimensional identity matrix. In Eq. (2B), k_δ is a constant of proportionality and η is a distributional parameter (or hyperparameter) to be assessed.

Prior information regarding the mixing coefficients B is quantified with a matrix normal distribution (Eq. (3A)), and prior information about the covariances of observations Σ with an inverted Wishart distribution (Eq. (3B)).

$$p(B|\Sigma) = (2\pi)^{-np/2}|D|^{-p/2}|\Sigma|^{-(q+2)/2}e^{-\mathrm{tr}\Sigma^{-1}(B-B_0)D^{-1}(B-B_0)'/2}, \tag{3a}$$

$$p(\Sigma) = k_\Sigma|\Sigma|^{-\nu/2}e^{-\mathrm{tr}\Sigma^{-1}Q/2}. \tag{3b}$$

The distributional parameters η, $B_0 = C$, $D = (X'X)^{-1}$, $\nu = n$, and $Q = (Y - XC')'(Y - XC')$ are estimated using an empirical Bayes approach that uses the current data ($C = Y'XD$ is the estimate of B found by regression). In Eq. (3B), k_Σ is a constant of proportionality. This is done with the multivariate regression of Eq. (1), resulting in a completely determined joint conjugate prior distribution. This regression also determines the maximum likelihood estimates of the parameters for the current FMRI dataset Y.

The joint likelihood of the FMRI observations Y is also given by the matrix normal distribution (Eq. (4)).

$$p(Y|X, B, \Sigma) = (2\pi)^{-np/2}|\Sigma|^{-n/2}e^{-\mathrm{tr}\Sigma^{-1}(Y-XB')'(Y-XB')/2}. \tag{4}$$

The joint conjugate prior distribution of the parameters (Eq. (5)) is the product of the prior distributions of these parameters (Eqs. (2) and (3)).

$$p(r, B, \Sigma, \delta) = p(r|\delta)p(\delta)p(B|\Sigma)p(\Sigma). \tag{5}$$

The joint likelihood and joint conjugate prior are formally combined using Bayes' rule to yield the joint posterior distribution of the parameters (Eq. (6)).

$$p(r, B, \Sigma, \delta|X, Y) \propto p(Y|X, B, \Sigma)p(r|\delta)p(\delta)p(B|\Sigma)p(\Sigma). \tag{6}$$

From the combined information contained in the posterior distribution (Eq. (6)), summary measures (such as voxel-specific means and covariances) can be obtained for each parameter of interest. A formal technique for doing this is by utilizing posterior marginal distributions [27]. However, it is impossible to analytically derive the marginal posterior distributions of r, B, Σ, or δ. An alternative strategy utilized here is to use a Markov Chain Monte Carlo (MCMC) method to numerically determine these functions from their posterior conditional distributions. The marginal posterior means estimates (denoted as r_{post}, δ_{post}, $B_{2\mathrm{post}}$ and Σ_{post}) are derived by iterative Gibbs sampling. Gibbs sampling, a stochastic integration algorithm, generates random variates $r_{(i)}$, $B_{(i)}$, $\Sigma_{(i)}$, and $\delta_{(i)}$ with i ranging from 1 to an integer $L + 5000$. The posterior conditional modes are used as the initial samples, which are then processed with 50 iterations of the iterated conditional mode algorithm, essentially a numerical hill-climbing of the error surface [29], to improve Gibbs Sampling convergence [27]. The output of ICM provides the initial values for Gibbs sampling $r_{(0)}$, $B_{(0)}$, $\Sigma_{(0)}$, and $\delta_{(0)}$. The first 5000 generated variates are discarded as stochastic equilibration, or "burn-in," and the last L are retained and then averaged to determine the final estimates for the marginal posterior means of the parameters (Eq. (7)). The posterior reference function r is estimated by r_{post} and δ_{post}, voxel-wise activation is assessed by the last column of posterior regression coefficients $B_{2\mathrm{post}}$, and the posterior variance-covariance matrix Σ_{post} is used to assess the interdependencies of drug responses between different voxels within the ROI. Prevalent and structured relationships in Σ_{post} indicate the presence of brain activity not modeled by the reference function.

$$r_{\mathrm{post}} = \bar{r} = \frac{1}{L}\sum_{i=1}^{L}\bar{r}_{(i)}, \tag{7a}$$

$$B_{\mathrm{post}} = \bar{B} = \frac{1}{L}\sum_{i=1}^{L}\bar{B}_{(i)}, \tag{7b}$$

$$\Sigma_{\text{post}} = \bar{\Sigma} = \frac{1}{L}\sum_{i=1}^{L} \bar{\Sigma}_{(i)}, \tag{7c}$$

$$\delta_{\text{post}} = \bar{\delta} = \frac{1}{L}\sum_{i=1}^{L} \bar{\delta}_{(i)}. \tag{7d}$$

The marginal posterior variance-covariance matrix of the posterior mean/mixing matrix B_{post} is obtained after constructing a vector of the posterior means and mixing coefficients [27].

$$b = \begin{bmatrix} B_1' & \dots & B_{q+2}' \end{bmatrix}', \tag{8}$$

$$\Psi = \frac{1}{L}\sum_{i=1}^{L} \bar{b}_{(i)}\bar{b}_{(i)}' - \bar{b}\bar{b}'. \tag{9}$$

Since the distribution of B_{post} was specified to be matrix normal (Eq. (3A)), the distribution of b, the stacked columns of B, is vector normal.

$$p(b|Y) \propto |\Psi|^{-1/2} e^{-(b-\bar{b})\Psi^{-1}(b-\bar{b})'/2}. \tag{10}$$

Since there is always interest in FMRI to assess the voxelwise significance of the calculated statistics, the marginal distribution of the vector b (Eq. (10)) is used to derive standard normal z-statistics. If Ψ_k is the kth $p \times p$ submatrix along the diagonal of Ψ, then it represents the covariance matrix of the multivariate normal B_k, the kth column of B.

$$p\left(B_k|\bar{B}_k, Y\right) \propto |\Psi_k|^{-1/2} e^{-(B_k-\bar{B}_k)'\Psi_k^{-1}(B_k-\bar{B}_k)/2}. \tag{11}$$

The marginal distribution of a scalar coefficient within B_k is normal (and any subset of coefficients within B_k is distributed as multivariate normal), from which statistical significance can be obtained. This assessment is of one regression coefficient of a single voxel, whose associated variance is the jth diagonal element of Ψ_k.

$$p\left(B_{kj}|\bar{B}_{kj}, Y\right) \propto (\Psi_{kj})^{-1/2} e^{-(B_{kj}-\bar{B}_{kj})^2/(2\Psi_{kj})}. \tag{12}$$

Finally, a z-score can be obtained from the results of Eq. (12), where z has a normal distribution with zero mean and unit variance.

$$z = \frac{B_{kj} - \bar{B}_{kj}}{\sqrt{\Psi_{kj}}}. \tag{13}$$

3. Experimental procedures

3.1. FMRI experiments

This human study was carried out in accord with the Declaration of Helsinki and approved by the Medical College of Wisconsin IRB. BOLD time series were collected from a cocaine-dependent human subject (male, right-handed, non-treatment seeking) as described previously [3]. All experiments were performed on a 1.5 Tesla scanner (GE Medical Systems, Milwaukee, WI). A hybrid MESBAC-EPI sequence (flip angle = 50°, TE = 30 ms, 5 mm slice thickness) was used to acquire whole-brain BOLD images. Briefly, the MESBAC technique acquires 4 images of each of 4 slices covering the midbrain and OFC with incremental changes in the z-gradient, and these images are combined in reconstruction to produce a composite, susceptibility-compensated image of the lower brain [23]. The MESBAC slices were acquired in an interleaved fashion with 16 single-shot EPI slices covering the remainder of the brain. The result is dramatically reduced distortion in OFC FMRI data, at the cost of temporal resolution (effective TR = 8 s). This tradeoff is feasible for pharmacological investigations, where drug-elicited changes in brain activity are expected to occur over many seconds [23].

The subject received a cocaine infusion and saline infusion in separate FMRI runs in random order. Each run lasted for 20 min, during which the entire brain was imaged every 8 s (150 time points). After seven minutes a single 20 mg/70 kg dose of cocaine (or control dose of saline of equal volume) was administered intravenously (IV) over 30 s.

High and *craving* ratings were given by the subject via joystick along a visual analog scale (VAS), following visual prompts that appeared on the screen throughout the scan. The VAS is a horizontal bar anchored at the left end with the words *least ever* and at the right end with *most ever.* Requesting the subject to make his or her own assessment of drug effects in relation to past experiences is accepted as reliable in studies of abused substances [30]. In addition to the FMRI runs, high-resolution whole-brain anatomical images were obtained.

3.2. Data analysis

The application of BSS is demonstrated below in multiple examples representing various circumstances (using the same FMRI experiment as the data source). The raw BOLD and anatomical data were preprocessed with a despiking algorithm and a rigid volumetric motion-correction algorithm in AFNI [31], then exported to Matlab (MathWorks, Natick, MA). The motion parameters were within the allowable range for MESBAC BOLD acquisition (less than 1.5 mm drift in any direction, and less than 1.5 ° rotation from base position).

The BOLD time series were then processed with BSS: the data matrix Y in Eq. (1) is comprised of the BOLD data, and X contains linear noise terms and the prior reference function r. The initial estimate of r is specific to the example, where Examples 1A, 2A, and 3 use a pharmacokinetic model, Example 1B uses the VAS *high* time series, and Example 2B uses BOLD data collected from anatomically and functionally connected brain regions. The size of the data matrix Y (and consequently the dimension n for the entire analysis) also changes between examples: Example 1 uses a single ROI (64 voxels), Example 2 uses four ROIs (144 voxels), and Example 3 processes an entire brain slice (724 voxels). The likelihood estimate of Y and the prior coefficients B are determined by multivariate linear regression. Following the application of Bayes' rule, the posterior estimates of r, δ, B, and Σ are determined by Gibbs sampling. For all examples the posterior regression coefficients B_2 represented the voxels of interest in a general brain-mapping sense: suprathreshold t-scores, derived via Eq. (12), are presented for comparison between prior and posterior B_2. Prior and posterior estimates of $r_0(t)$ are presented to illustrate the influence of the data Y on the reference functions. The posterior variance-covariance matrix Σ_{post} was converted into correlation statistics and displayed in a matrix; off-diagonal values of the matrix represented interaction between voxels found by BSS analysis. These values were summarized in Example 2A (as a percentage of significantly correlated pair of voxels, out of the total combinations of voxels belonging to different ROIs) to estimate interregional interaction. In Example 2B, the influence of one functionally-defined circuit on another was estimated by the posterior estimate of δ, which contained the covariance present between reference functions.

4. Demonstrations of BSS with acute cocaine BOLD data

4.1. Example 1. Single ROI under acute cocaine challenge

The chosen ROI is a 64-voxel region in the left medial OFC (Fig. 1A), an area conclusively related to cocaine-induced brain activity [3]. The shape of the BOLD signals in several voxels (Fig. 1B) appear to reflect the pharmacokinetic characteristics of cocaine, with a rapid rise time and a decay lasting several minutes. BSS was used to process this data using a reference function supplied by a pharmacokinetic model (Example 1A) and subject-reported VAS data (Example 1B). Maps of t-statistics were generated for voxel-by-voxel comparison between the two cases (Fig. 2).

4.1.1. Example 1A. Prior hemodynamic reference function based on a drug-response model

The prior reference function $r_0(t)$ is a γ-variate function estimating a two-compartment pharmacokinetic model: $r_0(t) = u(t)R_0t^6e^{-t/10}$, where R_0 is a scaling parameter, t is the peristimulus time ($t = 0$ at the start of the cocaine infusion), and $u(t)$ is a unit step function. This model assumes that the hemodynamic response to intravenous administration of cocaine is directly related to the absorption and clearance of the drug [22]. The rapid absorption of cocaine into the brain tissue from the blood following IV administration allows this assumption. Also, the relatively fast absorption and slower clearance of cocaine [32] justifies an approximate model with the γ-variate. A more complex model may be feasible with a higher time resolution in the BOLD data in future studies. The posterior regression coefficients demonstrate activation on the left side of the ROI (Fig. 2A), as might be expected when looking at the nonlinear signal changes present in the first four columns of the raw data matrix (Fig. 1). Also notable is that the limited amount of data has begun to add irregular fluctuations into the posterior reference function (Fig. 2B).

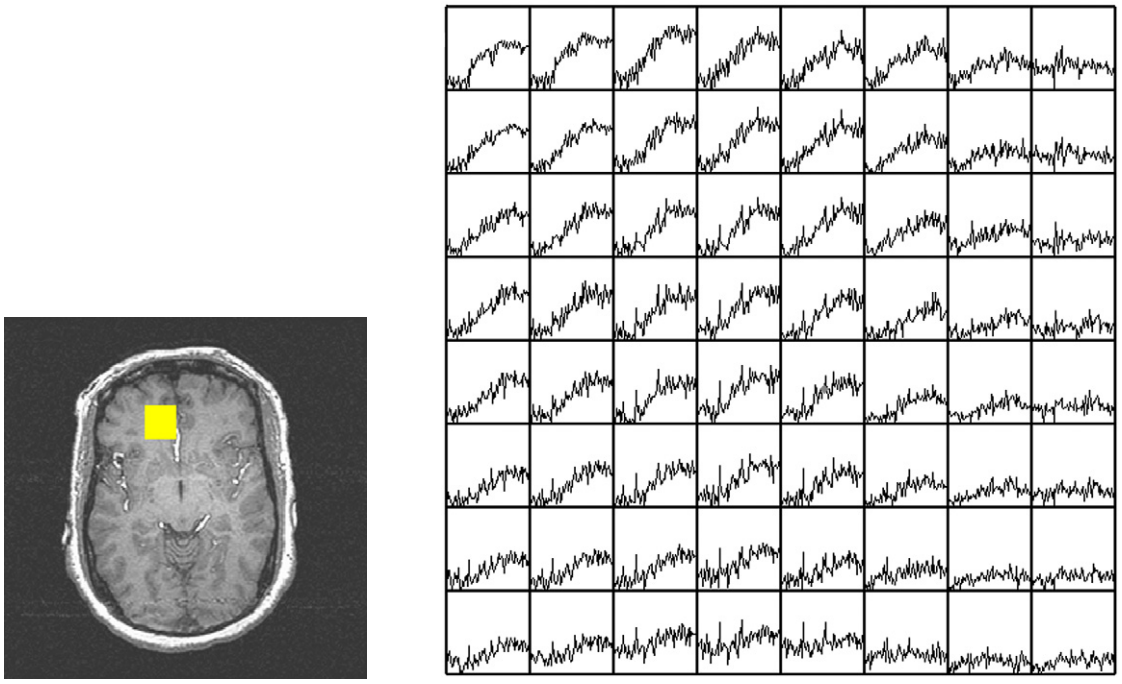

(A) (B)

Fig. 1. Raw data used in Example 1. (A) ROI of Example 1. 64 voxel timecourses are selected from an axial slice of the left medial orbital gyrus. The left side of the image corresponds to the left side of the subject's brain, as in all anatomy shown in subsequent figures (left is left). (B) Raw BOLD timecourses (149 observations) that make up Y. Note the contribution of linear noise terms and nonlinear BOLD signal changes presumed to correlate with intravenous BOLD infusioa.

4.1.2. Example 1B. Prior reference function based on concurrently measured subject rating data

The prior reference function $r_0(t)$ is a scaled time series acquired from a joystick controlled by the subject during the FMRI scan. The subject's *high* VAS ratings were interpolated with rectangular interpolation (Fig. 2D). A smaller proportion of the voxels exhibit significant activation t-scores for this model (Fig. 2C) than the pharmacokinetic model (Fig. 2A), demonstrating an advantage in sensitivity in using prior knowledge about the drug stimulus over subject-reported data.

4.2. Example 2. Multiple ROIs in the OFC

A mask was drawn defining 144 voxels that encompassed the ROIs: left medial orbital gyrus (BA 11), right orbital gyrus, left frontal pole (BA 10) and right posterior orbital gyrus (Fig. 3). These time series were extracted to Matlab and processed simultaneously with BSS.

4.2.1. Example 2A. Reference function based on a pharmacokinetic model of IV cocaine

First, BSS analysis was performed on the OFC data using a γ-function pharmacokinetic model as $r_0(t)$. Regression coefficients B_2 from the pre-Bayes' rule regression and the post-Bayes' rule regression are compared to demonstrate the impact of prior information on activation statistics (Fig. 4).

When the pharmacokinetic model is used as the reference function, the application of Bayes' rule results in a dramatically higher amount of successfully detected activated voxels (Figs. 4B and 4C). Regions 1 and 3 appear to be heavily correlated ($p < 0.01$ in 47% of voxel pairs), and the activated regions (1, 2, and 3) have notable intraregional correlation ($p < 0.01$ in 77, 70, and 64% of voxel pairs). This result is in agreement with a previously published multiple regression analysis to VAS time series [33], where the left medial OFC (Region 1) and left frontal pole (Region 3) both had a relation to the subjects' *high* ratings. It has been emphasized that common relationships to a reference function do not indicate that BOLD responses are correlated with each other [46]. Significant intervoxel correlations derived from the posterior Σ are not expected to fully agree with activation scores, and are in fact evidence

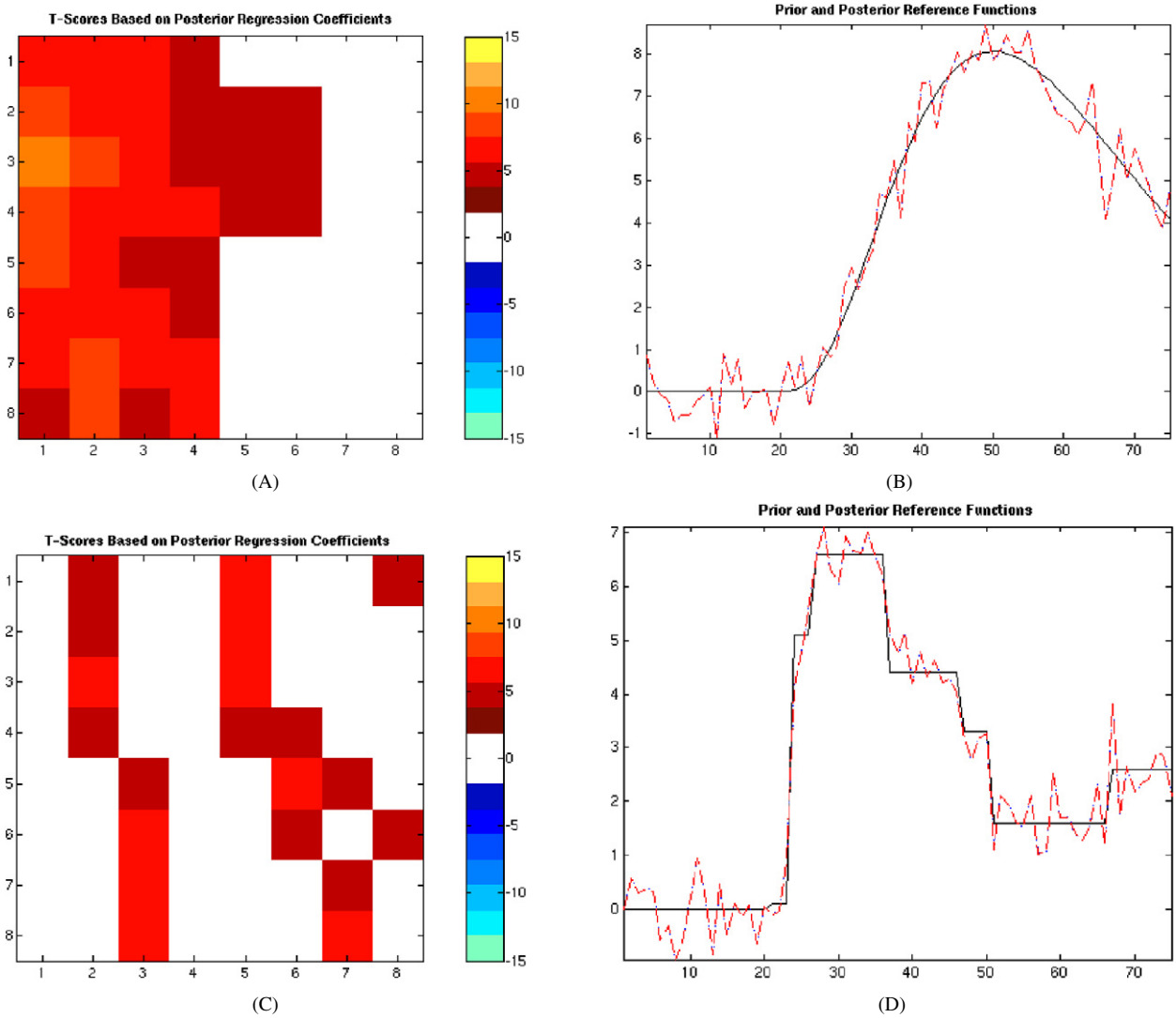

Fig. 2. Results from single ROI BSS analysis. (A) Example 1A regression coefficients. T-statistic map of ROI, based on posterior B_2 ($p < 0.01$). (B) Prior (solid) and posterior (dashed) reference functions in Example 1A. (C) Example 1B regression coefficients. T-statistic map of ROI, based on posterior B_2 ($p < 0.01$). (D) Prior (solid) and posterior (dashed) reference functions in Example 1B.

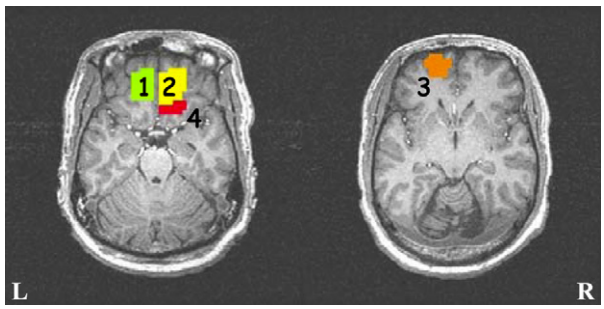

Fig. 3. OFC ROIs defined for Example 2 analysis. Regions are identified as (1) left medial orbital gyrus (BA 11), (2) right orbital gyrus, (3) left frontal pole (BA 10), and (4) right posterior orbital gyrus.

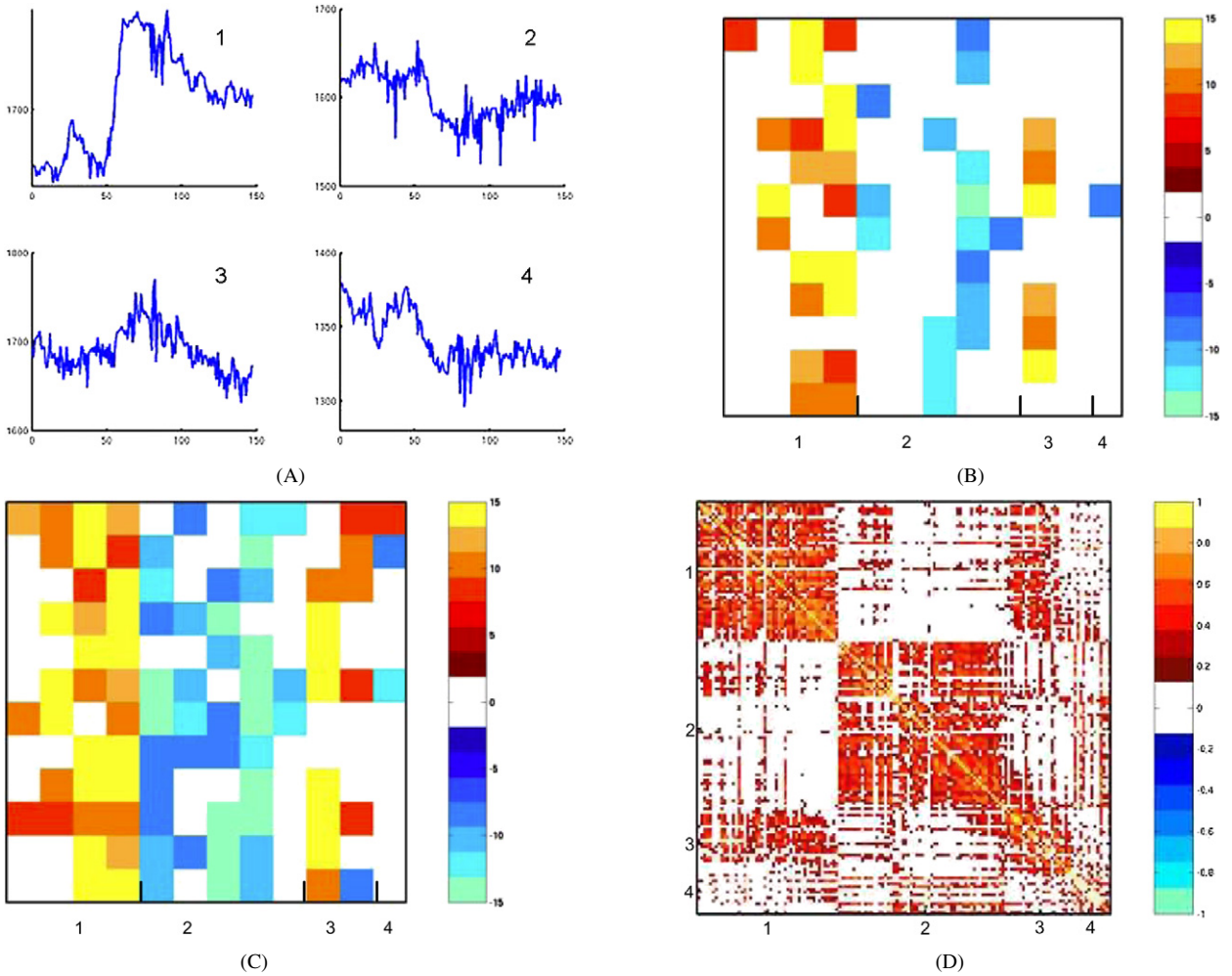

Fig. 4. Results of Example 2A. The regional BOLD data Y, regression coefficients B_2, which are interpreted as voxelwise activation statistics, and intervoxel correlation are grouped by region to depict the influence of anatomy on statistical results. (A) Mean raw BOLD time series for the four ROIs. The horizontal axes are the time point indexes and the vertical axes are BOLD magnitudes, which can be regarded as arbitrary units. (B) Compilation of t-scores calculated from the regression-generated prior estimate of B_2 ($p < 0.0001$), preceding the application of Bayes' rule. Each cell in the chart corresponds to a voxel belonging to one of the four ROIs. (C) Compilation of t-scores calculated from the posterior estimate of B_2 ($p < 0.0001$), following the application of Bayes' rule. The voxelwise t-scores in B and C are displayed in identical arrangements for visual comparison. (D) Correlation ($p < 0.01$) calculated from posterior estimate of Σ.

of incomplete modeling of the data by reference functions applied in univariate analysis. The negative BOLD signal in Region 2 also has highly correlated residuals (Fig. 4D), despite the fact that most of the voxels have high t-scores associated with a fit to the reference function (Fig. 4C).

4.2.2. Example 2B. Correlated reference functions derived from BOLD data of subcortical afferents

Another BSS analysis was performed using $r_0(t)$ derived from simultaneously acquired data in two functionally connected regions, the left nucleus accumbens (NAc) and left amygdala (Amy). The means of the reference functions were the means of the BOLD data acquired from the NAc and Amy (Fig. 5), and the prior variances were set to be equal, with zero cross-terms (Fig. 6, top). A necessary adjustment to the BSS algorithm comprised of replacing the matrix inversion steps with pseudoinverse calculations, extending the computation time but preventing the occurrence of ill-conditioned matrices.

The BSS analysis revealed an inverse correlation between posterior reference functions, illustrated by the off-axis contour plot of the reference function covariances (Fig. 6, bottom). The posterior confidence in the NAc reference

Fig. 5. Subcortical BOLD responses used as prior reference functions. (A) Mean BOLD response from the left NAc. (B) Mean BOLD response from the left Amy. These reference functions were calculated from BOLD data acquired simultaneously with the BOLD data forming the data matrix Y. The horizontal axes are the time point indexes and the vertical axes are BOLD magnitudes, which can be regarded as arbitrary units.

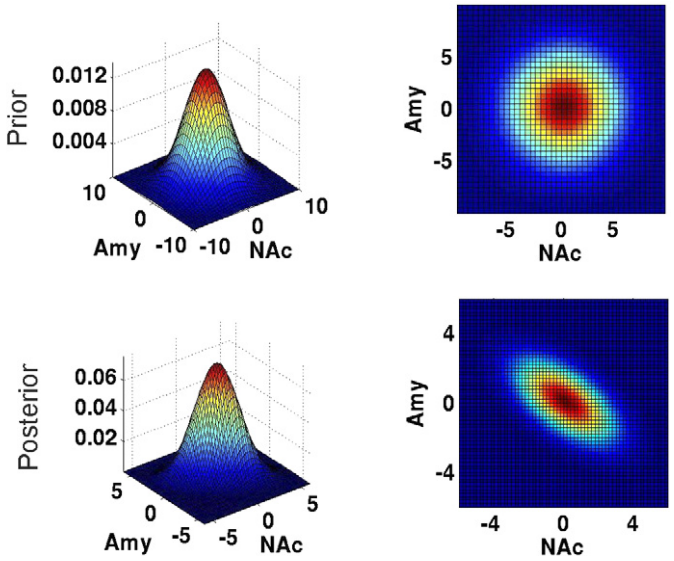

Fig. 6. Covariance parameters for prior and posterior reference functions for Example 2B. For illustration, reference means are set to zero. Each distribution is shown as a mesh diagram (left) and as a contour plot (right). Top row: Symmetric bivariate normal distribution derived from the prior assumption of equal and orthogonal variances. Bottom row: Asymmetric posterior distribution illustrating unequal confidence (with greater uncertainty associated with the Amy reference function) and cross-terms in the reference variance-covariance matrix δ_{post}.

function was much greater than that for the Amy reference function (resulting in the asymmetric distribution in Fig. 6), a result clearly predicted by the obvious difference in contrast-to-noise in the subcortical BOLD responses (Fig. 5).

Despite the relatively high posterior variance in the Amy reference function, the presence of cross-terms in the reference variance-covariance matrix δ_{post} implies that BSS analysis found evidence that both neural afferents influence the OFC cocaine response. Comparison of the prior and posterior activation maps (Fig. 7) reveals that the application of prior information via Bayes' rule improved the activation statistics for both NAc and Amy reference functions. The posterior NAc-activated OFC voxels exhibited higher z-scores than the prior results in the same locations (Fig. 7, top). The sparse prior Amy-related activation was improved following BSS with more activated voxels and higher z-scores (Fig. 7, bottom). Significant correlation was found between OFC BOLD responses, with blocks of heavy intercorrelation within anatomical regions (Fig. 8). Such structure in the data is assumed not to exist in more traditional FMRI analysis techniques.

4.3. Example 3. Processing of a larger dataset with eigenfactorization

The entire slice containing the OFC (excluding nonbrain and cerebellar voxels) was processed with BSS, to evaluate the capability of the method to process a larger set of voxels. The computation time for Examples 2A and 2B were approximately 90 and 120 min with Cholesky factorization, and matching results were achieved with eigenfactorization after approximately 3 and 5 h, respectively. The computation time associated with Example 3 and datasets of similar size (724 voxels) reached 15 h. All calculating was performed with an Intel 1.5 GHz processor system using 1 GB memory, running Matlab 6 (MathWorks, Natick, MA).

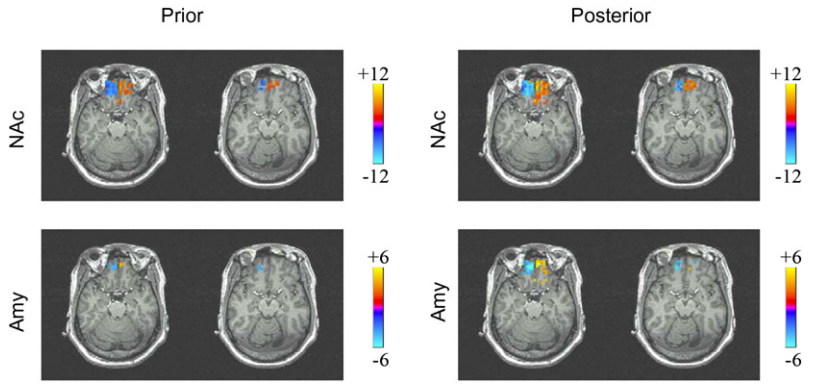

Fig. 7. Activation maps for Example 2B. For all maps, z-scores are presented with the threshold $z > 3.4$ (left is left). Top row: Activation maps for the NAc reference function. Bottom row: Activation maps for the Amy reference functioa left column: Activation maps calculated from regression parameters prior to the application of Bayes' rule. Right column: Activation maps calculated from the posterior regression coefficients $B_{2\text{post}}$.

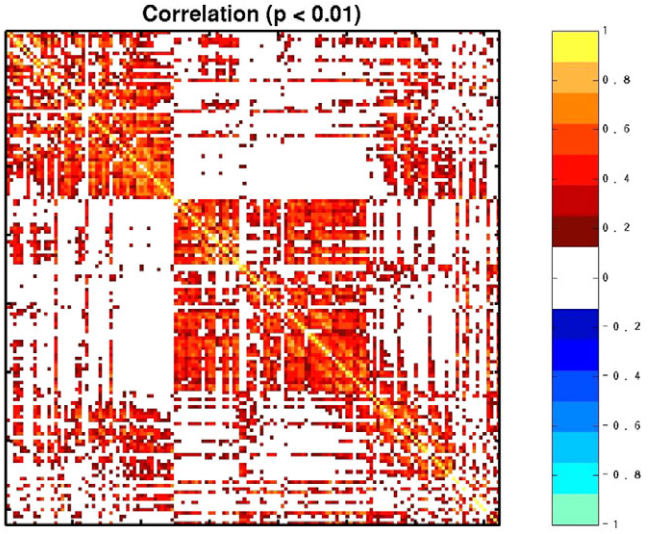

Fig. 8. Correlation between OFC voxels ($p < 0.01$). The correlation matrix was calculated from the posterior estimates Σ_{post} and sorted along the axes so that anatomical ROIs form blocks of rows/columns.

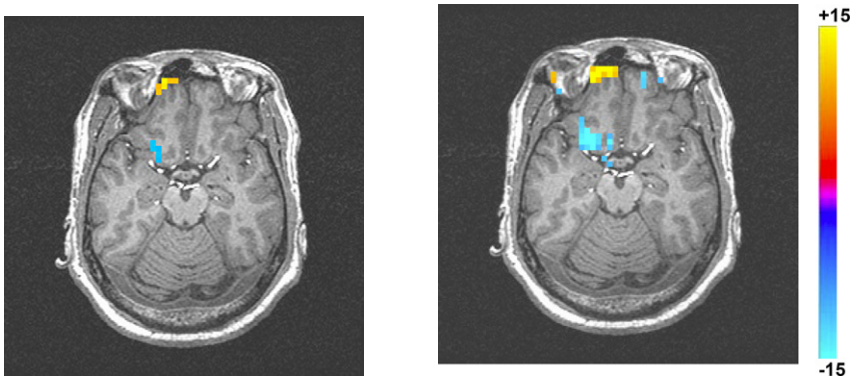

(A) (B)

Fig. 9. Regression coefficients of Example 3 mapped onto the OFC anatomy. (A) Regression coefficients prior to application of Bayes' rule (left is left). Both maps reflect the voxel threshold $t = 13.6$. The activation map reflects the good approximation that can be obtained from linear regression of the data. (B) Regression coefficients following application of Bayes' rule (left is left).

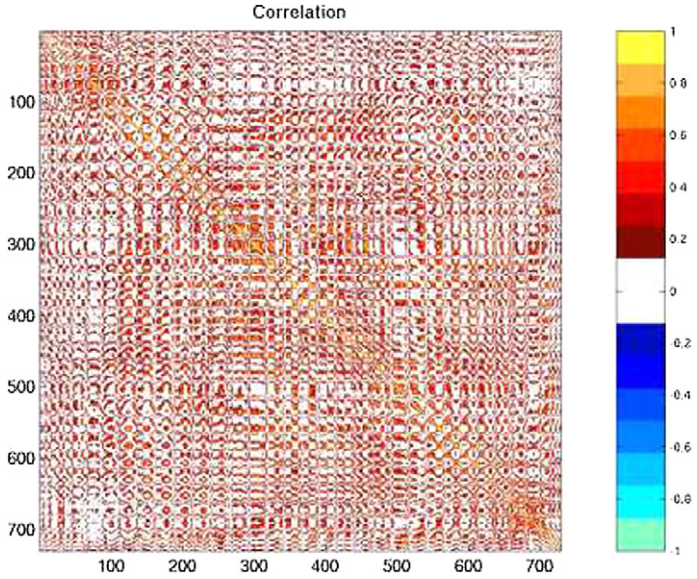

Fig. 10. Correlation matrix for 724-voxel region of Example 3. Threshold imposed at $p < 0.05$.

Figure 9 demonstrates additional voxels surpassing a stringent voxel threshold following the application of Bayes' rule. The left map (Fig. 9A) can be considered an initial guess based on the regression in BSS that is used to assess the hyperparameters. Groups of activated voxels appear in the left anterior medial OFC and left caudal OFC. Following application of Bayes' rule, both of these groups are larger in extent, and additional voxels appear in the right anterior medial OFC (Fig. 9B). The posterior covariances Σ_{post} were converted into correlation statistics and displayed in Fig. 10. As before, the region under investigation demonstrates significant spatial interdependencies, with positive correlation statistics passing the $p < 0.05$ threshold (Fig. 10).

5. Conclusions

The large interest in the development of multivariate analysis techniques is an acknowledgment of the richness of properly acquired BOLD FMRI time series. The fact that Bayesian source separation consistently detected structure in the residuals Σ_{post} of human cocaine BOLD data implies that exclusive study of low-frequency, sustained changes in BOLD data, as suggested earlier [6], omits some information germane to the classification of drug-sensitive brain regions. The quality of this information depends on the acquisition technique employed, as signal of higher frequency is generally more sensitive to noise. As susceptibility compensation and perfusion measurement techniques improve, multivariate analysis of FMRI time series stands to benefit from the inclusion of signal that would otherwise remain unaccounted in the residuals.

The benefits of using BSS include increased sensitivity to the drug-elicited BOLD response, shown in the posterior activation t-maps in Figs. 4, 7, and 9. More voxel activation scores passed the same threshold in the posterior map than in the prior map for all examples, and most voxels above the t threshold in the prior map had greater t-scores in the posterior map. However, the added sensitivity is heavily influenced by the choice of reference function, as shown in the Example 1 (Fig. 2). Greater sensitivity is an important advantage in acute drug FMRI studies, due to the limited pool of subjects and large expense that limit the size of the experiments [1,3]. Another advantage to using BSS is the ability to make probabilistic estimates of the interaction between voxels, contained in the posterior noise term Σ_{post}, and the posterior reference parameters r_{post} and δ_{post}. Posterior estimates of the reference functions could potentially be used to estimate the pharmacokinetic parameters of cocaine, information that has been previously linked to its abuse potential [32]. Interactions between the reference functions contained in δ_{post} could be used to infer a confluence of afferent signal sources. Such utilization of posterior probability information would be feasible in a study of several subjects.

Principal drawbacks to BSS are complexity and computation time. The replacement of Cholesky decomposition with eigenfactorization—a necessary step in order to process more voxels than time points within each BOLD time

series—resulted in noticeably longer processing. The computation time also appears to increase at a rate well above $O(n^2)$, where doubling the number of voxels to be processed more than doubles the processing involved.

Traditional FMRI data analysis techniques assume that intervoxel dependencies are not significant [12], or that they form "smoothness" in the data that allow parameterization akin to PET studies [34,35]. The fact that multivariate and Bayesian techniques [36–38] are increasingly adapted in FMRI analysis as computation power becomes available suggests a general willingness to depart from these assumptions.

Spatial ICA, which decomposes BOLD data into statistically independent components represented by single time-courses and regression-generated brain maps, has effectively replaced temporal ICA in the FMRI literature [39,40], and may be an interesting alternative to BSS in this application. Additionally, spatial ICA finds statistically independent component time series, a more stringent constraint than orthogonality. Further, in ICA the noise present in the BOLD data is not explicitly modeled [41]. Spatial ICA would likely enjoy more rapid convergence than BSS, but this advantage is heavily dependent on the strategy used to reduce the large initial dimension of BOLD data [41–43]. A thorough comparison of spatial ICA and BSS in processing drug-elicited BOLD responses is beyond the scope of the current study and would require data from multiple subjects. This is the topic of a planned forthcoming study.

The BSS technique, while computationally intense, provides flexibility in modeling the cocaine-induced hemodynamic response and related uncertainties yields a wealth of information related to the cross-dependencies between active voxels and sources. Additional examples of the application of BSS to pharmacological FMRI data have been previously presented [33,44,45,47].

Acknowledgments

This work was supported in part by the grants DA10214, RR00058, and MH019992. P.R.K. is currently supported by the NIH grant DA13649.

References

[1] H.C. Breiter, R.L. Gollub, R.M. Weisskoff, D.N. Kennedy, N. Makris, J.D. Berke, J.M. Goodman, H.L. Kantor, D.R. Gastfriend, J.P. Rorden, R.T. Mathew, B.R. Rosen, S.E. Hyman, Acute effects of cocaine on human brain activity and emotion, Neuron 19 (1997) 591–611.
[2] E.A. Stein, J. Pankiewicz, H.H. Harsch, J.-K. Cho, S.A. Fuller, R.G. Hoffmann, M. Hawkins, S.M. Rao, P.A. Bandettini, A.S. Bloom, Nicotine-induced limbic cortical activation in the human brain: A functional MRI study, Amer. J. Psychiatry 155 (1998) 1009–1015.
[3] P.R. Kufahl, Z. Li, R.C. Risinger, C. Rainey, A.S. Bloom, G. Wu, S.-J. Li, Neural responses to acute cocaine administration in the human brain detected by FMRI, Neuroimage 28 (2005) 914–924.
[4] E. Macaluso, C.D. Frith, J. Driver, Modulation of human visual cortex by crossmodal spatial attention, Science 289 (2000) 1206–1208.
[5] R. Henson, T. Shallice, R. Dolan, Neuroimaging evidence for dissociable forms of repetition priming, Science 287 (2000) 1269–1272.
[6] E.A. Stein, FMRI: A new tool for the in vivo localization of drug actions in the human brain, J. Anal. Toxicol. 25 (2001) 565–577.
[7] D.B. Rowe, A Bayesian approach to blind source separation, J. Interdisciplin. Math. 5 (2002) 49–76.
[8] B.R. Logan, D.B. Rowe, An evaluation of thresholding techniques in FMRI analysis, Neuroimage 22 (2004) 95–108.
[9] K. Worsley, K. Friston, Analysis of FMRI time series revisited again, Neuroimage 2 (1995) 173–181.
[10] S.D. Forman, J.D. Cohen, M. Fitzgerald, W.F. Eddy, M.A. Mintun, D.C. Noll, Improved assessment of significant activation in functional magnetic resonance imaging (FMRI): Use of a cluster-size threshold, Magn. Res. Med. 33 (1995) 636–647.
[11] K.C. Berridge, T.E. Robinson, What is the role of dopamine in reward: Hedonic impact, reward learning, or incentive salience? Brain Res. Brain Res. Rev. 28 (1998) 309–369.
[12] N. Lange, Statistical procedures for functional MRI, in: C.T.W. Moonen, P.A. Bandettini (Eds.), Functional MRI, second ed., Springer, Heidelberg, 1999, pp. 301–335.
[13] R. Gnanadesikan, Methods for Statistical Data Analysis of Multivariate Observations, second ed., Wiley, New York, 1997.
[14] K. Friston, C. Frith, P. Liddle, R. Frackowiak, Functional connectivity: The principal-component analysis of large (PET) data sets, J. Cereb. Blood Flow Metab. 13 (1993) 5–14.
[15] B. Biswal, J.L. Ulmer, Blind source separation of multiple signal sources of FMRI data sets using independent component analysis, J. Comp. Assist. Tomog. 23 (1999) 265–271.
[16] R.Z. Goldstein, N.D. Volkow, Drug addiction and its underlying neurobiological basis: Neuroimaging evidence for the involvement of the frontal cortex, Am. J. Psychiatry 159 (2002) 1642–1682.
[17] K.H. Knuth, Informed source separation: A Bayesian tutorial, in: B. Sankur, E. Cetin, E. Tekalp, E. Kuruoglu (Eds.), Proceedings of the 13th European Signal Processing Conference, 2005.
[18] D.B. Rowe, Bayesian source separation for reference function determination in FMRI, Magn. Res. Med. 46 (2001) 374–378.
[19] S.J. Press, Subjective and Objective Bayesian Statistics, second ed., Wiley, New York, 2003.
[20] T. Bayes, An essay towards solving a problem in the doctrine of chances, Philos. Trans. R. Soc. London 53 (1763) 370–418.
[21] P.M. Lee, Bayesian Statistics: An Introduction, Oxford Univ. Press, New York, 1989.

[22] E.A. Stein, R. Risinger, A.S. Bloom, Functional MRI in pharmacology, in: C.T.W. Moonen, P.A. Bandettini (Eds.), Functional MRI, second ed., Springer, Heidelberg, 1999, pp. 525–538.
[23] Z. Li, G. Wu, X. Zhao, F. Luo, S.-J. Li, Multiecho segmented EPI with z-shimmed background gradient compensation (MESBAC) pulse sequence for FMRI, Magn. Res. Med. 48 (2002) 312–321.
[24] S.J. Roberts, Independent component analysis: Source assessment and separation—A Bayesian approach, IEEE Proc. Vision Image Signal Process. 145 (1998) 149–154.
[25] K.H. Knuth, Bayesian source separation and localization, in: A. Mohammad-Djafari (Ed.), SPIE'98 Proceedings: Bayesian Inference for Inverse Problems, 1998, pp. 147–158.
[26] A. Mohammad-Djafari, A Bayesian approach to source separation, in: 19th Internation Workshop on Maximum Entropy and Bayesian Methods, 1999.
[27] D.B. Rowe, Multivariate Bayesian Statistics, Chapman & Hall/CRC Press, Boca Raton, FL, 2003.
[28] K.J. Friston, A.P. Holmes, K.J. Worsley, J.-B. Poline, C.D. Frith, R.S.J. Frackowiak, Statistical parametric maps in functional imaging: A general linear approach, Human Brain Mapp. 2 (1995) 189–210.
[29] D.V. Lindley, A.F.M. Smith, Bayes estimates for the linear model, J. R. Stat. Soc. B 34 (1972).
[30] M.W. Fischman, R.W. Foltin, Utility of subjective-effects measurements in assessing abuse liability of drugs in humans, British J. Addict. 86 (1991) 1563–1570.
[31] R.W. Cox, AFNI: Software for the analysis and visualization of functional magnetic resonance images, Comput. Biomed. Res. 29 (1996) 162–173.
[32] N.D. Volkow, Y.S. Ding, J.S. Fowler, G.J. Wang, J. Logan, J.S. Gatley, S. Dewey, C. Ashby, J. Liebermann, R. Hitzemann, A.P. Wolf, Is methylphenidate like cocaine? Studies on their pharmacokinetics and distribution in the human brain, Arch. Gen. Psychiatry 52 (1995) 456–463.
[33] P.R. Kufahl, D.B. Rowe, S.-J. Li, Exploring intervoxel dependencies in human pharmacological FMRI data, in: Proc. ISMRM 13th Sci. Meeting, Miami Beach, 2005, p. 1579.
[34] K.J. Friston, P. Jezzard, R. Turner, Analysis of functional MRI time-series, Human Brain Mapp. 1 (1994) 153–171.
[35] K.J. Friston, O. Josephs, E. Zarahn, A.P. Holmes, S. Rouquette, J.-B. Poline, To smooth or not to smooth? Neuroimage 12 (2000) 196–208.
[36] V.D. Calhoun, J.J. Pekar, V.B. McGinty, T. Adali, T.D. Watson, G.D. Pearlson, Different activation dynamics in multiple neural systems during simulated driving, Human Brain Mapp. 16 (2002) 158–167.
[37] K.J. Friston, W. Penny, C. Phillips, S. Kiebel, G. Hinton, J. Ashburner, Classical and Bayesian inference in neuroimaging: Theory, Neuroimage 16 (2002) 465–483.
[38] K.J. Friston, D.E. Glaser, R.N.A. Henson, S. Kiebel, C. Phillips, J. Ashburner, Classical and Bayesian inference in neuroimaging: Applications, Neuroimage 16 (2002) 484–512.
[39] M.J. McKeown, S. Makeig, G.G. Brown, T.-P. Jung, S.S. Kindermann, A.J. Bell, T.J. Sejnowski, Analysis of FMRI by blind separation into independent spatial components, Human Brain Mapp. 6 (1998) 160–188.
[40] V.D. Calhoun, T. Adali, G.D. Pearlson, J.J. Pekar, Spatial and temporal independent component analysis of functional MRI data containing a pair of task-related waveforms, Human Brain Mapp. 13 (2001) 43–53.
[41] M.J. McKeown, T.J. Sejnowski, Independent component analysis of FMRI data: Examining the assumptions, Human Brain Mapp. 6 (1998) 368–372.
[42] C.F. Beckmann, J.A. Noble, S.M. Smith, Investigating the intrinsic dimensionality of FMRI data for ICA, Neuroimage 13 (2001) S76.
[43] Z. Wang, J. Wang, V. Calhoun, H. Rao, J.A. Detre, A.R. Childress, Strategies for reducing large FMRI data sets for independent component analysis, Magn. Res. Imag. 24 (2006) 591–596.
[44] P.R. Kufahl, D.B. Rowe, S.-J. Li, A Bayesian hemodynamic drug response model for FMRI analysis, in: Proc. ISMRM 11th Sci. Meeting, Toronto, 2003, p. 1811.
[45] A.S. Bloom, R.G. Hoffman, S.A. Fuller, J. Pankiewicz, H.H. Harsch, E.A. Stein, Determination of drug-induced changes in functional MRI signal using a pharmacokinetic model, Human Brain Mapp. 8 (1999) 235–244.
[46] R. Baumgartner, R. Somorjai, R. Summers, W. Richter, L. Ryner, Correlator beware: Correlation has limited selectivity for fMRI data analysis, Neuroimage 12 (2000) 240–243.
[47] P.R. Kufahl, D.B. Rowe, S.-J. Li, Bayesian source separation of drug-indiced responses with correlated reference functions, in: ISMRM 14th Sci. Meeting, Seattle, 2006, p. 1160.

Peter R. Kufahl is currently a postdoctoral fellow at the Behavioral Neuroscience Laboratory in the Psychology Department at Arizona State University (ASU). He earned his B.S. degree in computer engineering at the Milwaukee School of Engineering in 1998, and his Ph.D. degree in biophysics at the Medical College of Wisconsin in 2006. In between these degrees he has worked in telecommunications engineering and advertising. He is currently supported by a Kirschstein-NRSA individual fellowship NIDA, researching animal models of cocaine addiction. He also teaches psychopharmacology at ASU.